JOURNAL OF THE ROYAL SOCIETY Interface

J. R. Soc. Interface (2011) **8**, 590–600
doi:10.1098/rsif.2010.0306
Published online 25 August 2010

Macromolecular dynamics in red blood cells investigated using neutron spectroscopy

Andreas Maximilian Stadler[1,*], Lambert van Eijck[2], Franz Demmel[3] and Gerhard Artmann[4]

[1]*Research Centre Jülich, 52425 Jülich, Germany*
[2]*Institut Laue-Langevin, 38042 Grenoble, France*
[3]*Rutherford Appleton Laboratory, Didcot OX11 0QX, UK*
[4]*Institute of Bioengineering, Aachen University of Applied Science, 52428 Jülich, Germany*

We present neutron scattering measurements on the dynamics of haemoglobin (Hb) in human red blood cells (RBCs) *in vivo*. Global and internal Hb dynamics were measured in the ps to ns time and Å length scales using quasi-elastic neutron backscattering spectroscopy. We observed the cross over from global Hb short-time to long-time self-diffusion. Both short- and long-time diffusion coefficients agree quantitatively with predicted values from the hydrodynamic theory of non-charged hard-sphere suspensions when a bound water fraction of around 0.23 gram H_2O per gram Hb is taken into account. The higher amount of water in the cells facilitates internal protein fluctuations in the ps time scale when compared with fully hydrated Hb powder. Slower internal dynamics of Hb in RBCs in the ns time range were found to be rather similar to results obtained with fully hydrated protein powders, solutions and *Escherichia coli* cells.

Keywords: haemoglobin; red blood cells; neutron spectroscopy; protein dynamics; macromolecular diffusion

1. INTRODUCTION

Ongoing research is dedicated to obtaining a coherent picture of the interactions and dynamical properties of proteins in their physiological environment. Cells are highly complex objects which are composed of organelles, tens of thousands of different proteins, RNA and DNA, lipids, polysaccharides and many other chemical components. Red blood cells (RBCs) in this sense are exceptional. They are highly specialized and relatively simple in their composition with the main macromolecular component, haemoglobin (Hb), making up 92 per cent of the dry weight. The concentration of Hb in RBCs is $c = 0.33\ \mathrm{g\ ml^{-1}}$ with a corresponding volume fraction of $\phi = 0.25$ [1]. The hydrodynamic radius of Hb is approximately 32 Å [2], and the average distance between Hb molecules is in the order of 1 nm [1]. RBCs are therefore particularly well-suited model systems to study the physical properties of concentrated protein solutions *in vivo*.

From a biological point of view the properties of human RBCs are interesting to study as well because they exhibit a variety of remarkable properties. RBCs have been shown to undergo a passage transition through narrow micropipettes at body temperature [3]. The single cells were aspirated with a micropipette (diameter of the pipette tip approx. 1.5 μm) and, at temperatures lower than body temperature, all cells blocked the pipette. Above body temperature all aspirated RBCs passed through the narrow micropipette tip easily without any apparent resistance. The passage temperature was 36.3 ± 0.3°C, which is remarkably close to human body temperature [3]. It was found that the passage behaviour is caused by a reduction in the viscosity of the concentrated Hb solution in the RBCs [3]. The loss of viscosity and the passage transition in the micropipette experiments were found to be connected to perturbations and partial unfolding of the structure of Hb at body temperature [4]. Further studies revealed that the structural perturbations of Hb at body temperature lead to Hb aggregation above approximately 37°C [2], and concomitantly RBCs release cytosolic cell water to the outside blood plasma as observed in colloid osmotic pressure measurements [5]. A direct correlation between the structural perturbation temperature of Hb and the body temperature of a large variety of different species was reported, which further supported the biological relevance of the effect [2,6]. It was speculated that the partial loss of Hb structure causes an increase in surface hydrophobicity, which might result in stronger protein–protein interactions and thus lead to protein aggregation above body temperature [2,7,8].

Krueger and co-authors [1,9] studied the interactions of Hb in RBCs and concentrated solution and demonstrated that a hard-sphere potential plus screened

*Author for correspondence (a.stadler@fz-juelich.de).

Electronic supplementary material is available at http://dx.doi.org/10.1098/rsif.2010.0306 or via http://rsif.royalsocietypublishing.org.

Received 6 June 2010
Accepted 4 August 2010

electrostatics can approximately describe the protein–protein interaction potential. The same results were also obtained later for concentrated myoglobin solutions [10]. It might be of interest to note that studies on concentrated solutions of crystallins and lysozyme demonstrated that a delicate balance between hard-sphere and weak attractive interactions are crucial for the stability of these concentrated protein solutions [11–13]. In further experiments, Doster & Longeville [14] examined the diffusion of Hb in RBCs using neutron spin-echo spectroscopy. The authors had the idea to interpret the diffusion of Hb in RBCs using the theory of colloidal diffusion at high concentration. The neutron spin-echo technique is sensitive to molecular motions occurring in the ns and nm time and length scales. Doster & Longeville [14] compared the measured short-time and long-time self-diffusion coefficient of Hb with theoretical calculations of non-charged hard-sphere suspensions with direct and hydrodynamic interactions. It was necessary to include the hydration shell as a hydrodynamic coat to account for the discrepancy with colloidal theory. Furthermore, it was deduced that hydrodynamic and not direct interactions dominate Hb diffusion at high concentration.

Without hydration water, proteins would neither fold correctly [15–17] nor acquire the conformational flexibility which is considered relevant for biological activity [18]. Motions in proteins occur over a very large range of time scales from fast reorientations of amino acid side chains in the ps range, to slower motions of the protein backbone in the ns time scale and to very slow processes of protein subunits and folding processes in the μs and ms range [19]. Fast fluctuations in the ps and ns time scales are considered to act as lubricants and to enable much slower physiologically important motions [20]. Hydration-dependent internal protein dynamics has been studied with incoherent neutron scattering in several model systems mainly as hydrated powders, including myoglobin [21,22], lysozyme [23–25] and α-amylase [26–28]. In incoherent neutron scattering experiments, the single particle motions of hydrogen (H) atoms are detected. H atoms are indicators of average protein dynamics as they constitute approximately 50 per cent of the atoms and are uniformly distributed in the macromolecules [29]. Hydration water not only enables protein dynamics but participates actively in protein function. Around 60 additional water molecules are bound in the hydration layer of the oxygenated form of Hb as compared with the deoxygenated state of Hb [30]. The additional water molecules were found to be thermodynamically important for regulation of Hb activity. The study carried out by Colombo and co-workers [31] was done in an aqueous solution at a Hb concentration of 64 mg ml^{-1}. Further studies revealed that binding of the extra water molecules is the rate-limiting step of Hb activity. Therefore, an important question is whether protein dynamics is adapted to the specific hydration level in cells.

In this paper, we present a study of Hb dynamics in RBCs in the ps to ns time- and Å length scales using high-resolution quasi-elastic neutron scattering (QENS). The aim of the study is to demonstrate how QENS allows the measurement and separation of internal protein dynamics and global macromolecular diffusion in whole cells. The QENS technique provides complementary information to fluorescent correlation spectroscopy [32,33] or neutron spin-echo spectroscopy [14,34,35], which are sensitive to different time–space windows of protein fluctuations.

2. MATERIAL AND METHODS

2.1. Sample preparation

Samples of human venous blood from healthy adults were drawn into tubes containing heparin to prevent blood coagulation. RBC samples were prepared as described in Stadler *et al.* [7]. During the sample preparation, the RBCs were gassed with CO to increase the stability of Hb and the glycocalyx matrix was removed. The cells were washed several times with D_2O 4-(2-hydroxyethyl)-1-piperazineethanesulphonic acid (HEPES) buffer (137 mM NaCl, 4 mM KCl, 1.8 mM $CaCl_2$, 0.8 mM Na_2HPO_4, 0.2 mM NaH_2PO_4, 0.7 mM $MgSO_4$, 8.4 mM HEPES and 4 mM NaOH) at pD = 7.4 and 290 mOsm to reduce the neutron scattering contribution of the buffer. The washing steps were repeated until the level of H_2O was estimated to be below 0.1 vol.%. The shape of the cells was checked with optical microscopy after the washing steps. The cell pellet was sealed in a flat aluminium sample holder of 0.2 mm thickness for the neutron scattering experiment. It was checked by weighing that there had been no loss of sample material during the experiment.

2.2. Dynamic light scattering experiments

Samples for the dynamic light scattering experiments were prepared from a drop of blood taken from the finger tip. The RBCs were washed with H_2O HEPES buffer and lysed with distilled water. The sample for dynamic light scattering experiments was not gassed with CO. Before the dynamic light scattering experiments, the dilute Hb solution in H_2O buffer (0.1 M KCl, 61.3 mM K_2HPO_4, 5.33 mM KH_2PO_4, pH 7.4, 290–300 mOsm) was centrifuged at 20 000 relative centrifugal force and filtered using 0.25 μm nitrocellulose filters. UV/VIS absorption spectroscopy was used to determine the concentration of the Hb solution. The Hb was found to be in the oxy-state as evidenced by the characteristic bands in the absorption spectrum, and the protein concentration was 0.4 mg ml^{-1}. The protein concentration was determined using extinction coefficients of 13.8 $mM^{-1} \times cm^{-1}$ at 541 nm and 128 $mM^{-1} \times cm^{-1}$ at 405 nm for oxy-Hb; the molar concentration is per haem group [36]. Dynamic light scattering of dilute human Hb solution was measured on a Wyatt DAWN-EOS instrument (Wyatt Technology, Santa Barbara, CA) and corrected for temperature-dependent D_2O viscosity using literature values [37]. The diffusion coefficients were calculated using the Astra 5 software package from the manufacturer. Around 5 ml of sample was measured per experiment.

2.3. Neutron scattering experiments

Neutron scattering was measured on the high-resolution neutron backscattering spectrometers IN10 and IN16 at the ILL (http://www.ill.eu/instruments-support/instruments-groups/yellowbook/) and IRIS at the ISIS spallation source (http://www.isis.stfc.ac.uk/instruments/iris/). To minimize multiple scattering, RBC samples with high transmissions were used (0.95 on IN16 and IRIS and 0.9 on IN10). The instruments IRIS, IN10 and IN16 are characterized by energy resolutions ΔE of 17, 1 and 0.9 μeV (FWHM), respectively, which correspond to slowest observable motions in the order of $\Delta t = \hbar/\Delta E$ of approximately 40 ps and 1 ns, respectively. Neutron scattering was measured in the range of $0.49 \leq q \leq 1.6$ Å^{-1} on IN16, $0.5 \leq q \leq 1.45$ Å^{-1} on IN10 and $0.48 \leq q \leq 1.6$ Å^{-1} on IRIS, where q is the modulus of the scattering vector. The instrumental energy resolution was determined with a vanadium measurement. The scattering contribution of the empty aluminium sample holder was subtracted from the measured data. Neutron detectors were grouped on IN16 and IRIS to obtain better statistics. Incoherent scattering of D_2O solvent contributes partially to the measured intensities: free and interfacial water dynamics are out of the Å-ns space and time window of IN10 and IN16 and contribute only as a flat background to the measured spectra [38]. Experimental data are dominated by Hb motions on the IRIS spectrometer, and the incoherent contribution of D_2O on IRIS is estimated to be smaller than 4 per cent at $q < 1.3$ Å^{-1} [7]. Gaspar *et al.* [39] evaluated the coherent and incoherent scattering contributions of concentrated protein solutions in D_2O solvent. In a completely dry myoglobin powder the authors found an incoherent scattering fraction of approximately 90 per cent and a coherent scattering fraction of approximately 10 per cent between 0.5 and 1.5 Å^{-1}. For a concentrated myoglobin solution of 360 mg ml^{-1}, the authors reported an incoherent scattering fraction of around 80 per cent and a coherent scattering fraction of around 20 per cent between 0.5 and 1.5 Å^{-1}. The coherent scattering fraction of D_2O in the 360 mg ml^{-1} solution therefore has to be approximately 10 per cent in that scattering vector range. In RBCs the protein concentration is 330 mg ml^{-1} and the values should be comparable.

3. QENS DATA ANALYSIS

The scattering function of internal protein dynamics $S_I(q,\omega)$ can be written in a simplified form as an elastic term and a single Lorentzian that represents internal protein diffusive motions [29]

$$S_I(q,\omega) = A(q)\cdot\delta(\omega) + (1-A(q))\cdot\frac{1}{\pi}\cdot\frac{\Gamma_I(q)}{\omega^2+\Gamma_I(q)^2}. \tag{3.1}$$

The prefactor $A(q)$ is called the *elastic incoherent structure factor* (EISF), q is the modulus of the scattering vector and $\Gamma_I(Q)$ are the half-widths at half-maximum (HWHM) of the Lorentzian. The q-dependence of the EISF contains information about the geometry of localized motions, and the scattering vector dependence of $\Gamma_I(q)$ provides information about the diffusion coefficients and residences times of diffusive motions.

Global macromolecular diffusion consists of translational and rotational diffusions of the protein. The scattering function of global protein diffusion $S_G(q,\omega)$ is the convolution of the scattering functions of translational and rotational diffusions assuming that rotational and translational diffusions are uncorrelated. It was shown theoretically by Perez *et al.* [40] that rotational diffusion of a protein leads to an additional broadening of the measured HWHM. The scattering function $S_G(q,\omega)$ could be approximated by a single Lorentzian with the half-widths $\Gamma_G(q)$,

$$S_G(q,\omega) = \frac{1}{\pi}\cdot\frac{\Gamma_G(q)}{\omega^2+\Gamma_G(q)^2}. \tag{3.2}$$

The line-widths and the apparent diffusion coefficient D_{app} of the protein are related by $\Gamma_G(q) = D_{app}\cdot q^2$ [40]. The apparent diffusion coefficient D_{app} was compared with D_0, which is the translational diffusion coefficient of the protein at infinite dilution. The identical value of $D_{app}/D_0 = 1.27$ was obtained for myoglobin and haemoglobin [7,40]. The calculation of the contributions of rotational and translational diffusions to the measured spectra is described in appendix A.

Furthermore, it is assumed that internal protein dynamics and global protein diffusion are uncorrelated in concentrated protein solutions. The scattering function $S(q,\omega)$ then is the convolution between $S_I(q,\omega)$ and $S_G(q,\omega)$, $S(q,\omega) = S_I(q,\omega)\otimes S_G(q,\omega)$ [41]. The scattering function reads as

$$S(q,\omega) = \exp(-\langle x^2\rangle q^2)\cdot\left\{\frac{A(q)}{\pi}\cdot\frac{\Gamma_G(q)}{\Gamma_G(q)^2+\omega^2} + \frac{1-A(q)}{\pi}\cdot\frac{\Gamma_G(q)+\Gamma_I(q)}{[\Gamma_G(q)+\Gamma_I(q)]^2+\omega^2}\right\}, \tag{3.3}$$

where the exponential represents a Debye–Waller factor for fast molecular vibrations. $S(q,\omega)$ plus linear background was convoluted with the instrumental resolution function and fitted to the measured QENS spectra in the energy range of $-14 \leq E \leq +14$ μeV for IN16, $-12.4 \leq E \leq +12.4$ μeV for IN10 and $-0.5 \leq E \leq +0.5$ meV for IRIS using the DAVE software package [42].

Gaspar *et al.* [43] demonstrated that the half-widths of internal motions $\Gamma_I(q)$ are a weaker parameter than the EISF. The authors could fit measured QENS spectra equally well with constant or freely varying line-widths as a function of the scattering vector. As a test we fixed the line-widths of internal motions to the q-independent average value of $\Gamma_I(q) = 0.2$ meV. The obtained line-widths $\Gamma_G(q)$ of global Hb diffusion were then found to increase linearly with q^2 as expected but did not intercept zero at $q^2 \to 0$. A non-zero intercept at $q^2 \to 0$ of global protein diffusion is difficult to interpret with global Hb diffusion. On the other hand, when the line-widths $\Gamma_I(q)$ were allowed to vary freely,

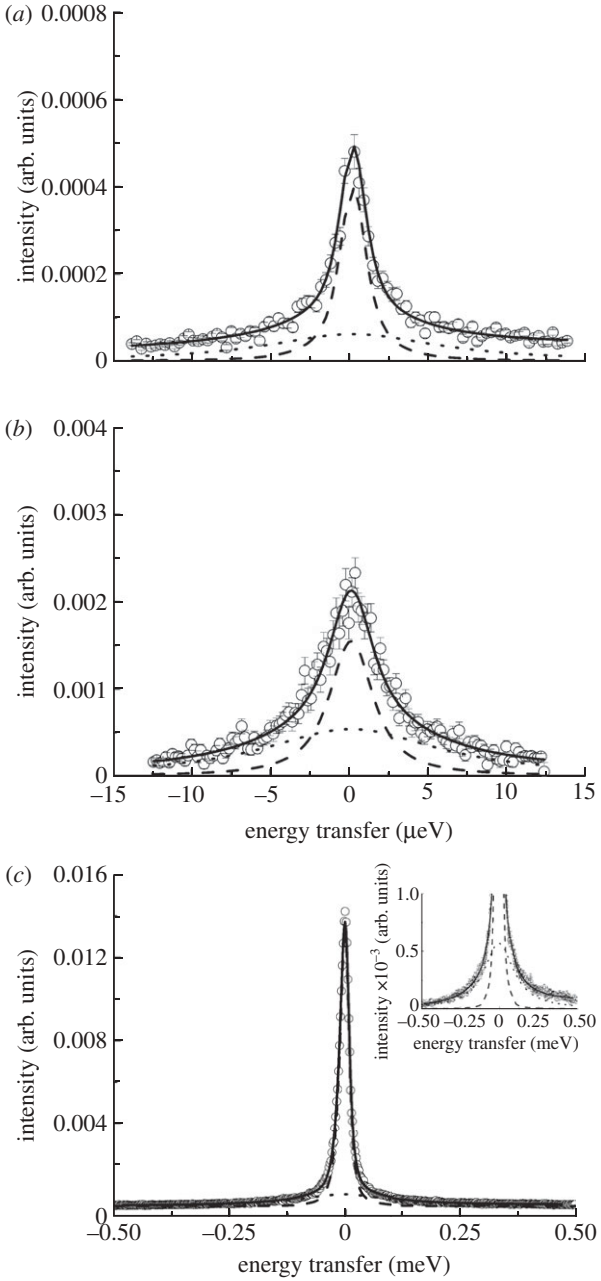

Figure 1. Experimental QENS data of Hb in RBCs measured on (*a*) IN16 at 11.9°C and $q = 1.3$ Å^{-1}, (*b*) IN10 at 19.1°C and $q = 1.45$ Å^{-1} and (*c*) IRIS at 16.9°C and $q = 1.37$ Å^{-1}. The solid black line is the total fit, and the dashed and the dotted lines represent, respectively, the narrow and broad Lorentzians used for data analysis. The inset in (*c*) on the right-hand side shows a magnification of the spectrum measured on IRIS to illustrate the quality of the fit. The instruments IRIS, IN10 and IN16 are characterized by energy resolutions ΔE of 17, 1 and 0.9 μeV (FWHM), respectively.

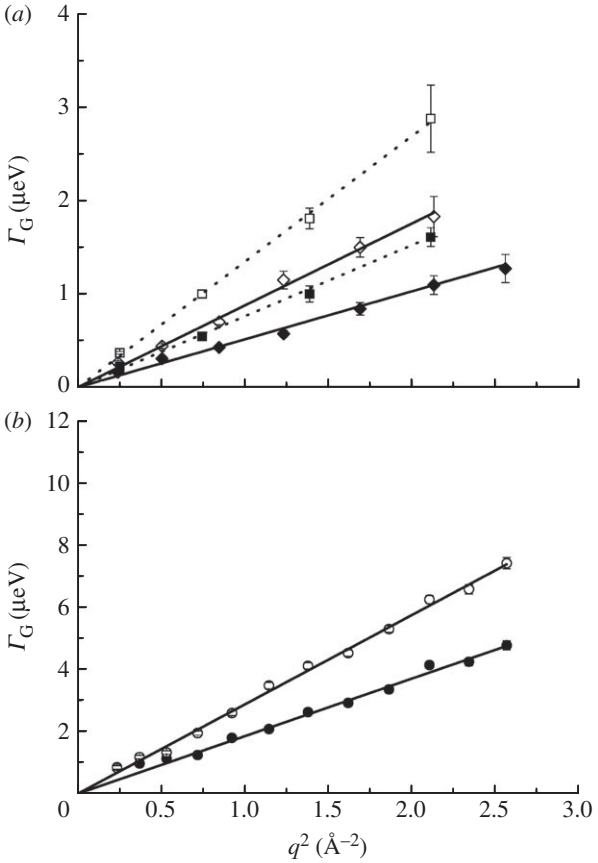

Figure 2. Half-widths at half-maximum of the Lorentzians of global Hb diffusion in RBCs measured with QENS on (*a*) IN16 (diamonds), IN10 (squares) (open square, 36.5°C, open diamond, 26.9°C; filled square, 19.1°C; filled diamond, 11.9°C) and (*b*) IRIS (open circle, 36.9°C; filled circle, 16.9°C). The straight lines are linear fits to the data. In (*a*) the solid lines are fits to IN16 and the dotted lines are fits to IN10 data. The linear increase of the line-widths with q^2 is a clear sign of continuous global Hb diffusion. The diffusion coefficients of Hb were determined from the slope of the linear fits. IN10 and IN16 are sensitive to motions in the time scale of approximately ns, whereas IRIS detects motions in the time scale of approximately 40 ps.

we obtained line-widths $\Gamma_G(q)$ that pass through zero as expected for global protein diffusion.

4. RESULTS AND DISCUSSION

In the following we present and discuss the results of our experiments. Typical QENS data measured on the neutron spectrometers IN16, IN10 and IRIS are shown in figure 1. The measured spectra were well described with a narrow and a broad Lorentzian for global macromolecular diffusion and internal Hb dynamics, respectively. First, we discuss the results about global Hb diffusion. Our interpretation follows the ideas of Doster & Longeville [14].

4.1. Global macromolecular diffusion

The measured HWHM for global Hb diffusion are presented in figure 2. Apparent diffusion coefficients D_{app} were determined according to $\Gamma_G(q) = D_{app} \cdot q^2$ in the range of $0.24 \leq q^2 \leq 2.56$ Å^{-2} for IN10 and IN16 data, and in the range of $0.72 \leq q^2 \leq 2.57$ Å^{-2} for IRIS data. The line-widths $\Gamma_G(q)$ of global Hb diffusion increase linearly with q^2 up to around 2.6 Å^{-2}. This behaviour is a clear sign of continuous global diffusion of Hb. The D_{app} contains a component of both translational and rotational diffusions of Hb. It was shown previously [7,40] that rotational diffusion of Hb leads to an additional broadening of the spectra by a

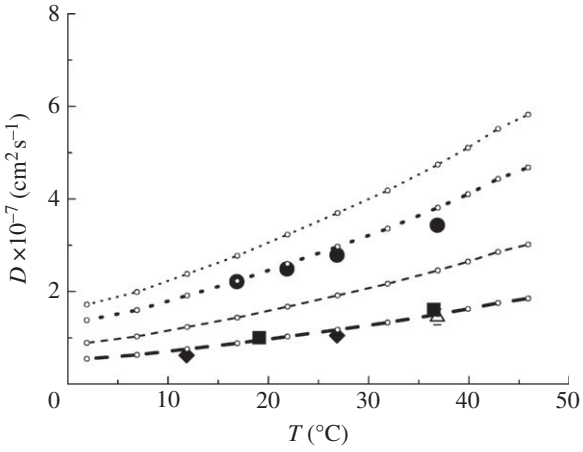

Figure 3. Diffusion coefficient D of Hb in RBCs as a function of temperature. The diffusion coefficients were measured with QENS on IRIS (circles), on IN16 (diamonds), on IN10 (squares) and with neutron spin-echo spectroscopy on IN15 (triangle) [14]. D_0 was measured with dynamic light scattering and scaled data points are given as small empty circles. The thin dotted and the thin dashed line show the theoretical values of short-time D_S^S and long-time self-diffusion D_S^L of Hb at a volume fraction of $\phi = 0.25$ with hydrodynamic interactions ($D_S^S = 0.56 \cdot D_0, D_S^L = 0.28 \cdot D_0$) [47]. The thick dotted and the thick dashed line represent the theoretical values for short-time and long-time self-diffusion of Hb assuming that a hydration layer of 0.23 gram H_2O per gram protein is bound to the surface of Hb. Experimental data agree well with the theoretical considerations when the bound hydration water layer is taken into account ($D_S^S = 0.45 \cdot D_0, D_S^L = 0.18 \cdot D_0$) [47].

factor of 1.27. Therefore, the apparent diffusion coefficients D_{app} were divided by 1.27 to obtain the global translational diffusion coefficient D of Hb. The essential steps in the calculation of the contributions of rotational and translational diffusions to the experimental spectra are outlined in appendix A. All obtained values of D are compared in figure 3. The line-widths obtained from the measurements with IN16 and IN10 intercept zero (figure 2*a*), which indicates that on time scales of approximately 1 ns global Hb diffusion does not sense confinement of neighbouring proteins. The $\Gamma_G(q)$ measured on IRIS appear to converge towards a plateau at small q^2 and low temperature (figure 2*b*). The feature indicates a cage effect of the neighbouring molecules on Hb diffusion in the ps time scale and has been observed before [7]. Multiple scattering might lead to a deviation from linear behaviour at small q^2. However, as the transmission of the sample was 0.95 multiple scattering should be completely negligible. An alternative explanation could be that small uncertainties of the resolution function might result in a plateau at small q^2, as the HWHM are only approximately 10 per cent of the energy resolution of IRIS. An observation time-dependent diffusion coefficient is obtained. Unruh *et al.* [44] observed a similar phenomenon. The authors studied the motions in liquid medium-chain *n*-alkanes using QENS with observation times from 1.1 to 900 ps and molecular dynamics simulations. The study revealed a time-dependent diffusion coefficient, and there was no need to use the obtained half-widths at low-resolution for the analysis of the high-resolution data. To check the validity of our interpretations, we have also performed a complementary analysis in time–space (see electronic supplementary material). The obtained diffusion coefficients in time–space and in energy–space are identical within the error bars. If the diffusion coefficient measured with IRIS is visible with IN16/IN10, we would obtain a mixture in time–space of the IRIS and the IN16/IN10 energy–space results. This is not the case and our check therefore demonstrates the validity of our analysis.

Studies on average macromolecular dynamics in *Escherichia coli* cells [45] and in concentrated myoglobin solutions [46] using high-resolution neutron backscattering spectroscopy reported that the measured line-widths of global macromolecular diffusion deviate from linear behaviour and tend towards saturation at large q^2. Jump-diffusion of the macromolecules was discussed as a possible explanation [45,46], as this mechanism would result in a saturation of the line-widths at large q^2. On the other hand, a distribution of diffusion coefficients could also be responsible for the deviation of the line-widths from linear behaviour [46]. Importantly, any kind of non-localized diffusion leads to line-widths that tend towards zero with $\Gamma_G(q) = D_{app} \cdot q^2$ at small q^2-values. Jasnin *et al.* [45] studied average macromolecular dynamics in *E. coli* using the IRIS spectrometer. Global macromolecular diffusion in *E. coli* was too slow and could not be resolved with IRIS. Prokaryotic cells, such as *E. coli*, are very complex objects which contain a vast amount of large macromolecular assemblies, such as ribosomes with a molecular mass of 2.5 MDa. Average macromolecular dynamics in *E. coli* are therefore difficult to attribute to a certain component. Hb is the main macromolecular component of RBCs with a rather small molecular mass of 65 kDa. It is reasonable to assume that global diffusion of Hb is significantly faster than that of large macromolecular complexes in *E. coli*, which would explain why Hb global diffusion in RBCs is visible on IRIS.

Tokuyama & Oppenheim [47] evaluated the short-time D_S^S and long-time D_S^L self-diffusion coefficients of concentrated non-charged hard-sphere suspensions with hydrodynamic and direct interactions as a function of the volume fraction ϕ and of the diffusion coefficient at infinite dilution D_0. Short-time self-diffusion corresponds to particles that move in a static configuration of the neighbouring particles at times $t < \tau_D$, with the structural relaxation time τ_D. The long-time limit of self-diffusion is reached at $t > \tau_D$. The values of the short- and long-time self-diffusion coefficients are equal only in dilute solution. At higher concentrations short-time self-diffusion is always faster than long-time self-diffusion. We measured the diffusion coefficient D_0 of Hb at infinite dilution with dynamic light scattering. The theoretical values of D_S^S and D_S^L of Hb at a volume fraction of $\phi = 0.25$ ($D_S^S = 0.56 \cdot D_0, D_S^L = 0.28 \cdot D_0$) are given in figure 3 [47]. It is obvious that the measured diffusion coefficients are too small and do not agree with the theoretical values. Full hydration of myoglobin

corresponds to a value of $h \sim 0.39$ gram H_2O per gram Mb [18]. It is believed that the critical hydration, to allow the onset of anharmonic motions in myoglobin (Mb), is around $h_{Mb} = 0.35$ gram H_2O per gram Mb [22]. Hb has a larger radius of gyration than Mb (Hb: $R_G \sim 24$ Å; Mb: $R_G \sim 16$ Å) and a smaller surface to volume ratio (S/V) [10,48]. Approximating Hb and Mb as spherical particles, the critical hydration of Hb should be around $h_{Hb} = (S/V)_{Hb}/(S/V)_{Mb} \times h_{Mb} =$ 16 Å/24 Å × 0.35 gram H_2O per gram Mb = 0.23 gram H_2O per gram Hb. It is known that the density of protein hydration water is approximately 10 per cent larger than the bulk solvent [49]. The partial specific volume ν of Hb plus hydration water is then $\nu = (0.75 + 0.23/1.1)$ ml $g^{-1} = 0.98$ ml g^{-1}, which corresponds to an effective volume fraction of Hb plus hydration water of $\phi = c \cdot \nu = 0.32$ with the concentration $c = 0.33$ g ml^{-1} of Hb in RBCs [14,50]. The measured self-diffusion coefficients of Hb with IN16, IN10 and IRIS agree with high accuracy with the theoretical values of Hb plus the hydration shell ($D_S^S = 0.45 \cdot D_0, D_S^L = 0.18 \cdot D_0$; [47]). In a study on the short-time limit of Hb diffusion in RBCs we estimated that the structural relaxation time τ_D is of the order of several hundred ps [7]. Therefore, IRIS is sensitive to motions which are faster than τ_D and short-time self-diffusion is detected. The high-resolution instruments IN16 and IN10, and neutron spin-echo spectroscopy [14], measure motions which are longer than τ_D, and the long-time limit of Hb self-diffusion is observed. We showed previously that, although approximately 90 per cent of cell water in RBCs has properties similar to bulk water, a small fraction of approximately 10 per cent cellular water exhibits strongly reduced dynamics and was attributed to water molecules which are bound to the surface of Hb [51]. The ratio of water per Hb in RBCs is $h \sim 2.3$ gram H_2O per gram Hb and an approximately 10 per cent fraction corresponds to a bound water fraction of approximately 0.23 gram H_2O per gram Hb, which is identical to the value reported in this article. Furthermore, Doster & Longeville [14] measured the diffusion of Hb in whole RBCs using spin-echo spectroscopy in the ns and nm time and length scales. The authors demonstrated that the presence of the hydration shell leads to a reduction in the diffusion coefficient of Hb. Garcia de la Torre [52] calculated hydrodynamic properties of proteins from atomic structures. It was demonstrated by comparing the calculated and experimental values that a hydration shell of $h \sim 0.27$ gram H_2O per gram Hb is bound to the surface of Hb. Our result is reasonably close to that value.

4.2. Internal haemoglobin dynamics

We now turn our attention to the results concerning internal protein dynamics. Detailed information about protein internal motions can be extracted from the scattering vector dependence of the quasi-elastic broadening and the EISF. The HWHM of internal protein dynamics measured on IN16 and on IRIS are given in figure 4*a*,*b*. The $\Gamma_I(q)$ measured with IRIS show typical behaviour of localized jump-diffusion. The half-widths tend towards a constant value at small q^2, which indicates confining effects of local boundaries. Diffusive jumps with a finite jump-length lead to a plateau in the line-widths at large scattering vectors. In the q^2-range of 0.72 and 2.57 $Å^{-2}$ the $\Gamma_I(q,\omega)$ measured on IRIS could be well described with a jump-diffusion model given by $\Gamma_I(q,\omega) = D_I q^2/(1 + D_I q^2 \tau)$ [41]. The parameters of the jump-diffusion model are the residence time before a jump τ and the jump-diffusion coefficient D_I of protein internal motions. In figure 5, the jump-diffusion coefficients and the residence times of internal Hb dynamics in RBCs are compared with jump-diffusion coefficients and residence times of internal Hb dynamics as hydrated powder ($h = 0.4$ gram D_2O per gram Hb) and as concentrated solution ($h = 1.1$ gram D_2O per gram Hb). The corresponding hydration level in RBCs is $h \sim 2.5$ gram D_2O per gram Hb. The results of the experiments with the hydrated Hb powder and concentrated Hb solution have been published before and are given here for comparison [8]. The Hb powder and solution were measured on neutron time-of-flight spectrometers with energy resolutions of 50 and 100 μeV, respectively. All data were analysed in the same way. The results demonstrate that an increase in the hydration level from one hydration shell in the Hb powder to around three hydration layers in the concentrated Hb solution increases the jump-diffusion

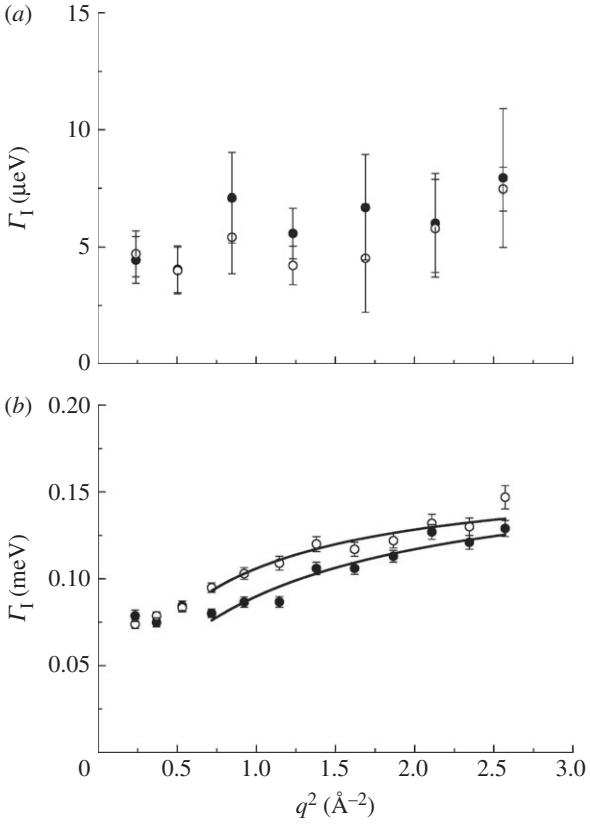

Figure 4. Half-widths at half-maximum of the $\Gamma_I(q)$ of internal Hb dynamics as a function of q^2. Data in (*a*) were measured on IN16 (open circle, 26.9°C; filled circle, 11.9°C) and (*b*) on IRIS (open circle, 36.9°C; filled circle, 16.9°C). The scattering vector dependence of the line-widths contains information on the observed motions in Hb. Solid lines in (*b*) are fits with a jump-diffusion model in the q^2-range from 0.72 to 2.57 $Å^{-2}$.

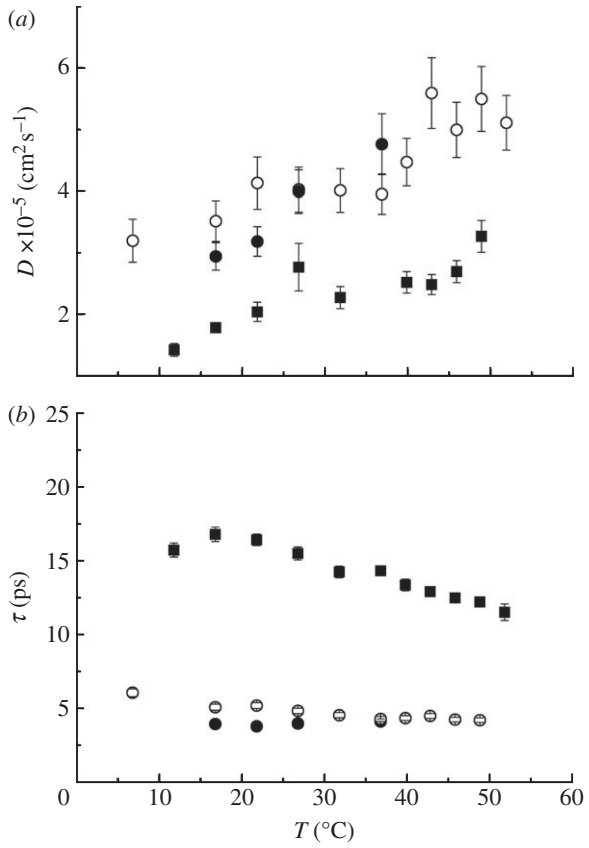

Figure 5. (*a*) Diffusion coefficients of internal motions in Hb as a function of temperature. Results from fully hydrated Hb powder, solution and Hb in RBCs at different hydration levels are compared. (*b*) Residence times of internal jump-diffusion as a function of temperature of the different samples. Hb in RBCs was measured on IRIS at ISIS (energy resolution 17 μeV), concentrated Hb solution on TOFTOF at FRM-II (resolution 100 μeV) and hydrated Hb powder on FOCUS at PSI (resolution 50 μeV; filled circle, Hb in RBCs; open circle, Hb $h = 1.1$ gram D_2O per gram Hb; filled square, Hb $h = 0.4$ gram D_2O per gram Hb).

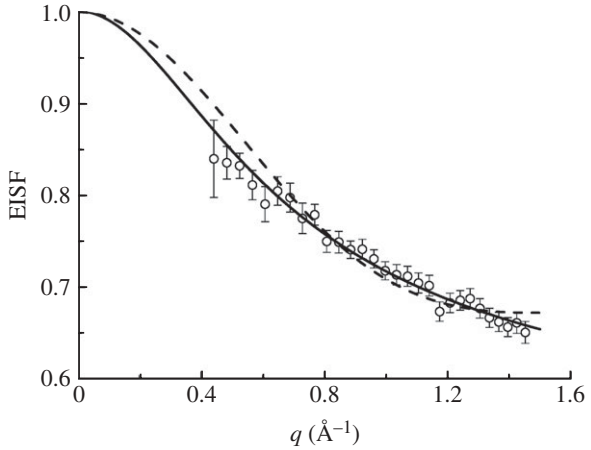

Figure 6. Elastic incoherent structure factor of Hb in RBCs measured on IRIS at a temperature of 26.9°C. The dashed line is a fit with the model for diffusion in a sphere. The solid line is a fit with the model for diffusion in a sphere with a Gaussian distribution of sphere radii.

coefficients and strongly reduces the residence times of internal protein dynamics in the ps time scale. A further increase in the hydration level to around six hydration layers per Hb in whole RBCs neither enhances the jump-diffusion coefficients nor reduces significantly the residence times as compared with the concentrated Hb sample. The rate of internal jump-diffusion in the ps time scale appears to be already fully developed in the concentrated Hb solution. The observed motions in the ps range could correspond to diffusive jumps of amino acid side chains and attached methyl groups [53].

The half-widths of internal protein dynamics from the experiment on IN16 are independent of the scattering vector within the error bars, as shown in figure 4*a*, and have average values of 5.8 ± 1.4 μeV at 11.9°C and 6.2 ± 1.0 μeV at 26.9°C. The line-widths determined with IN10 are 5.5 μeV at 19.1°C and 4.2 μeV at 36.5°C. The $\Gamma_1(q)$ on each individual spectrum of IN10 had large errors. The average value was used for all spectra at one temperature and held constant during fitting of IN10 data; the obtained values are rather imprecise and are given only for completeness.

The line-widths obtained on IN16 and IN10 are in agreement with other studies which investigated protein dynamics in the ns time scale using high-resolution quasi-elastic neutron scattering. Fitter *et al.* [54] studied hydrated bacteriorhodopsin and obtained half-widths of 5.5 μeV; Orecchini *et al.* [55] investigated hydrated β-lactoglobulin powder and found half-widths of 16 μeV; Busch *et al.* [46] found line-widths of 10 μeV of myoglobin in concentrated solution; and Jasnin *et al.* [45] measured average dynamics in whole *E. coli* and obtained line-widths of approximately 7 μeV. If we exclude the lactoglobulin case, the values of the measured line-widths are rather similar, although the hydration levels in the investigated systems are different. We recall that correlation times τ and line-widths Γ are inversely related by $\tau_{cor} = 1/\Gamma$. This seems to indicate that correlation times of motions in globular and membrane proteins in the ns time scale are rather similar in hydrated protein powders, solutions and in whole cells. As the observed line-widths on IN16 and IN10 are independent of the scattering vector, a different class of motions is observed using the high-resolution instruments. Rotational motions lead to line-widths which are independent of the scattering vector [41], and the observed dynamics might be attributed to slow rotations of side chains or relaxations of the protein backbone.

Information about the geometry of motions can be extracted from the measured EISF. Only four and six data points are available on IN10 and IN16, respectively. This is too few and does not allow an accurate analysis. Therefore, we limit our discussion to the results of the experiment using the IRIS spectrometer. The EISF obtained with IRIS at 26.9°C is shown in figure 6. The EISF was interpreted with the model of Volino & Dianoux [56] for diffusion in a sphere. The diffusion in a sphere model can be written as $A_0(q) = p + (1 - p) \cdot [3j_1(qa)/qa]^2$, where $j_1(qa)$ is the first-order spherical Bessel function of the first kind, a is the sphere radius and $A_0(q)$ is the EISF. The hydrogen atoms which appear immobile and mobile within

the instrumental energy resolution are represented by the fractions p and $(1-p)$, respectively. The obtained sphere radius a increases from 2.8 ± 0.1 Å at 16.9°C to 3.3 ± 0.1 Å at 36.9°C. The immobile fraction p has an average value of 0.67. These values reasonably agree with the results on macromolecular dynamics in *E. coli*, which found $a = 3.1$ Å and $p = 0.61$ at 6.9°C, and $a = 3.4$ Å and $p = 0.56$ at 26.9°C [45].

To take into account the heterogeneity of internal protein dynamics, Perez *et al.* [40] extended the diffusion in a sphere model and introduced a Gaussian distribution of sphere radii $f(a)$ instead of a single sphere. The Gaussian distribution is defined as $f(a) = 2/\sigma\sqrt{2\pi}\exp(-a^2/2\sigma^2)$, with the standard deviation σ as the free parameter. The mean value of the sphere radius is given by $\hat{a} = \sigma\sqrt{2/\pi}$. A neutron scattering study using specific isotope labelling in order to investigate the dynamics of specific amino acids in bacteriorhodopsin demonstrated the heterogeneity of internal protein dynamics [57]. The obtained average sphere radius $\hat{a}$ increases from $\hat{a} = 2.1 \pm 0.1$ Å at 16.9°C to $\hat{a} = 3.0 \pm 0.2$ Å at 36.9°C. The immobile fraction p has an average value of 0.50 and increases only slightly with temperature from $p = 0.47 \pm 0.02$ at 16.9°C to $p = 0.55 \pm 0.01$ at 36.9°C. Using the same model, we have quantified the average amplitudes of motion in concentrated Hb solution [8]. The average sphere radius was found to increase from $\hat{a} = 2.3$ Å at 6.9°C to $\hat{a} = 2.6$ Å at 36.9°C, while the immobile fraction was constant with temperature $p = 0.38$ [8]. Within the error bars the obtained average sphere radii of Hb in RBCs and of Hb in concentrated solution are similar when we exclude the value at 36.9°C, which is larger in Hb in RBCs than in the Hb solution. Although the energy resolutions of the instruments used for both experiments are different (17 and 100 μeV, respectively) the observed motions look similar. This might be either because the same motions are seen using the IRIS and the time-of-flight spectrometers or because different classes of motions in the order of 40 ps and several ps are similar. The second possibility would also imply that the corresponding hierarchical structures in the energy landscape are similar.

The model for diffusion in a sphere approximately describes the measured EISF. Better fits can be obtained when a Gaussian distribution of sphere radii is used. It should be noted that both the diffusion in a sphere model and the Gaussian distribution can only be simple and rough representations for the heterogeneity of internal protein dynamics. In any case, models are never wrong, they are just more or less appropriate.

5. CONCLUSION

In summary, we measured the global self-diffusion and internal dynamics of Hb in RBCs, *in vivo*, using high-resolution quasi-elastic neutron backscattering spectroscopy. It is demonstrated that global protein diffusion and internal dynamics can be separated and interpreted quantitatively. The cross over from the short- to the long-time limit of Hb self-diffusion could be observed. It is demonstrated that the diffusion of Hb at high concentration in RBCs can be described with concepts of colloid physics. Experimental data are in quantitative agreement with hydrodynamic theory of non-charged hard-sphere suspensions when it is assumed that the hydration shell moves with the protein. It is shown that interfacial protein hydration water has a strong influence on global protein diffusion under physiological conditions in cells. The same result was obtained by Doster & Longeville [14] using spin-echo spectroscopy. Experiments with whole RBCs using micropipette aspiration and colloidal osmotic pressure measurements [3,5] indicated that the cellular environment might have similarities to a colloidal gel. It was suggested that the trigger for the formation of the gel could be Hb–Hb interactions, which are influenced by the molecular properties of Hb [2,6]. Recently, we studied Hb–Hb interactions in concentrated solution using small-angle neutron scattering and showed that Hb molecules associate into a large-scale superstructure at high concentration [58]. In this article, we observe a slowing down of the atomistic diffusion of Hb, which might indeed lead to gel-like properties on a macroscopic scale. It is demonstrated how incoherent neutron scattering can contribute to the understanding of cellular phenomena on a macroscopic scale.

Internal Hb dynamics was also measured and could be separated from global Hb diffusion. The internal motions of Hb were compared with results obtained with hydrated powder and solution samples. Different types of motions were brought into focus by using neutron spectrometers with specific energy resolutions. Hydration water was found to have a strong influence on motions in the ps time scale. Jump-diffusion coefficients of internal Hb fluctuations are significantly enhanced and residence times of the internal diffusive jumps are reduced in RBCs as compared with fully hydrated Hb powder. Slower internal dynamics of Hb in RBCs in the ns time range were found to be rather similar to results obtained with fully hydrated protein powders, solutions and *E. coli* cells. Still missing is a combined analysis of the data measured with different spectrometers, which should be done in a future study. Future work might also be dedicated to investigating protein dynamics in whole cells under different environmental conditions.

The author (A.M.S.) thanks Georg Büldt for continuous support. We also thank Giuseppe Zaccai for valuable discussion and critical reading of the manuscript.

APPENDIX A. GLOBAL Hb DIFFUSION: CONTRIBUTION OF ROTATIONAL AND TRANSLATIONAL DIFFUSIONS

Global protein diffusion consists of translational and rotational protein diffusions around the centre of mass. Free translational diffusion is described by the scattering function

$$S_{\mathrm{trans}}(q,\omega) = \frac{1}{\pi} \cdot \frac{\Gamma_{\mathrm{trans}}(q)}{\omega^2 + \Gamma_{\mathrm{trans}}(q)^2}, \qquad (\mathrm{A}\,1)$$

with the diffusion coefficient $\Gamma_{\mathrm{trans}}(q) = D_0 \cdot q^2$ [41]. It was shown theoretically by Perez *et al.* [40] that rotational diffusion of a protein leads to an additional broadening of the measured HWHM. Rotational and translational diffusions of the protein are assumed to be uncorrelated. In that case, the scattering function of global protein diffusion $S_{\mathrm{G}}(q,\omega)$ is the convolution of the scattering functions of translational and rotational diffusions

$$\begin{aligned} S_{\mathrm{G}}(q,\omega) &= S_{\mathrm{trans}}(q,\omega) \otimes S_{\mathrm{rot}}(q,\omega) \\ &= \frac{1}{\pi} \cdot \sum_{l=0}^{\infty} B_l(q) \\ &\quad \times \frac{\Gamma_{\mathrm{trans}}(q) + \Gamma_l(q)}{\omega^2 + [\Gamma_{\mathrm{trans}}(q) + \Gamma_l(q)]^2}, \end{aligned} \tag{A 2}$$

with $\Gamma_l = l\,(l+1) \cdot D_{\mathrm{rot}}$ and the rotational diffusion coefficient D_{rot} [40]. The integrals in the terms $B_0(q)$ and $B_l(q)$ are extensions of the Sears [59] model for rotation on the surface of a sphere. They describe the distribution of hydrogen atoms within the protein

$$\left.\begin{aligned} B_0(q) &= \textstyle\int_{r=0}^{R} 4\pi r^2 \cdot j_0^2(qr)\,\mathrm{d}r, \\ B_{l\geq 1}(q) &= \textstyle\int_{r=0}^{R} 4\pi r^2 \cdot (2l+1) \cdot j_l^2(qr)\,\mathrm{d}r. \end{aligned}\right\} \tag{A 3}$$

The terms j_l are the lth-order spherical Bessel function of the first kind and R is the radius of the Hb. The terms $B_l(q)$ were integrated numerically and the obtained scattering function $S_{\mathrm{G}}(q,\omega)$ could be perfectly approximated by a single Lorentzian with the apparent diffusion coefficient D_{app} and the HWHM $\Gamma_{\mathrm{G}}(q) = D_{\mathrm{app}} \cdot q^2$. The apparent diffusion coefficient D_{app} was compared with D_0, which gave the relation of $D_{\mathrm{app}}/D_0 = 1.27$ [7,40].

REFERENCES

1 Krueger, S. & Nossal, R. 1988 SANS studies of interacting hemoglobin in intact erythrocytes. *Biophys. J.* **53**, 97–105. (doi:10.1016/S0006-3495(88)83070-4)

2 Digel, I., Maggakis-Kelemen, C., Zerlin, K. F., Linder, P., Kasischke, N., Kayser, P., Porst, D., Temiz Artmann, A. & Artmann, G. M. 2006 Body temperature-related structural transitions of monotremal and human hemoglobin. *Biophys. J.* **91**, 3014–3021. (doi:10.1529/biophysj.106.087809)

3 Artmann, G. M., Kelemen, C., Porst, D., Büldt, G. & Chien, S. 1998 Temperature transitions of protein properties in human red blood cells. *Biophys. J.* **75**, 3179–3183. (doi:10.1016/S0006-3495(98)77759-8)

4 Artmann, G. M., Burns, L., Canaves, J. M., Temiz-Artmann, A., Schmid-Schonbein, G. W., Chien, S. & Maggakis-Kelemen, C. 2004 Circular dichroism spectra of human hemoglobin reveal a reversible structural transition at body temperature. *Eur. Biophys. J.* **33**, 490–496. (doi:10.1007/s00249-004-0401-8)

5 Artmann, G. M. *et al.* 2009 Hemoglobin senses body temperature. *Eur. Biophys. J.* **38**, 589–600. (doi:10.1007/s00249-009-0410-8)

6 Zerlin, K. F. T., Kasischke, N., Digel, I., Maggakis-Kelemen, C., Artmann, A. T., Porst, D., Kayser, P., Linder, P. & Artmann, G. M. 2007 Structural transition temperature of hemoglobins correlates with species' body temperature. *Eur. Biophys. J.* **37**, 1–10. (doi:10.1007/s00249-007-0144-4)

7 Stadler, A. M., Digel, I., Artmann, G. M., Embs, J. P., Zaccai, G. & Buldt, G. 2008 Hemoglobin dynamics in red blood cells: correlation to body temperature. *Biophys. J.* **95**, 5449–5461. (doi:10.1529/biophysj.108.138040)

8 Stadler, A. M., Digel, I., Embs, J. P., Unruh, T., Tehei, M., Zaccai, G., Büldt, G. & Artmann, G. M. 2009 From powder to solution: hydration dependence of human hemoglobin dynamics correlated to body temperature. *Biophys. J.* **96**, 5073–5081. (doi:10.1016/j.bpj.2009.03.043)

9 Krueger, S., Chen, S. H., Hofrichter, J. & Nossal, R. 1990 Small angle neutron scattering studies of HbA in concentrated solutions. *Biophys. J.* **58**, 745–757. (doi:10.1016/S0006-3495(90)82417-6)

10 Longeville, S., Doster, W. & Kali, G. 2003 Myoglobin in crowded solutions: structure and diffusion. *Chem. Phys.* **292**, 413–424. (doi:10.1016/S0301-0104(03)00292-1)

11 Cardinaux, F., Gibaud, T., Stradner, A. & Schurtenberger, P. 2007 Interplay between spinodal decomposition and glass formation in proteins exhibiting short-range attractions. *Phys. Rev. Lett.* **99**, 118301. (doi:10.1103/PhysRevLett.99.118301)

12 Dorsaz, N., Thurston, G. M., Stradner, A., Schurtenberger, P. & Foffi, G. 2009 Colloidal characterization and thermodynamic stability of binary eye lens protein mixtures. *J. Phys. Chem. B* **113**, 1693–1709. (doi:10.1021/jp807103f)

13 Stradner, A., Foffi, G., Dorsaz, N., Thurston, G. & Schurtenberger, P. 2007 New insight into cataract formation: enhanced stability through mutual attraction. *Phys. Rev. Lett.* **99**, 198103. (doi:10.1103/PhysRevLett.99.198103)

14 Doster, W. & Longeville, S. 2007 Microscopic diffusion and hydrodynamic interactions of hemoglobin in red blood cells. *Biophys. J.* **93**, 1360–1368. (doi:10.1529/biophysj.106.097956)

15 Chaplin, M. 2006 Opinion: do we underestimate the importance of water in cell biology? *Nat. Rev. Mol. Cell Biol.* **7**, 861–866. (doi:10.1038/nrm2021)

16 Cheung, M. S., Garcia, A. E. & Onuchic, J. N. 2002 Protein folding mediated by solvation: water expulsion and formation of the hydrophobic core occur after the structural collapse. *Proc. Natl Acad. Sci. USA* **99**, 685–690. (doi:10.1073/pnas.022387699)

17 Dobson, C. M., Sali, A. & Karplus, M. 1998 Protein folding: a perspective from theory and experiment. *Angew. Chem. Int. Ed.* **37**, 868–893. (doi:10.1002/(SICI)1521-3773(19980420)37:7<868::AID-ANIE868>3.0.CO;2-H)

18 Rupley, J. A. & Careri, G. 1991 Protein hydration and function. *Adv. Prot. Chem.* **41**, 37–172. (doi:10.1016/S0065-3233(08)60197-7)

19 McCammon, J. A. & Harvey, S. C. 1987 *Dynamics of proteins and nuclear acids*. Cambridge, UK: Cambridge University Press.

20 Brooks, C. L., Karplus, M. & Pettitt, B. M. 1988 *Proteins: a theoretical perspective of dynamics, structures, and thermodynamics*, vol. 71. New York, NY: Wiley.

21 Doster, W. 2008 The dynamical transition of proteins, concepts and misconceptions. *Eur. Biophys. J.* **37**, 591–602. (doi:10.1007/s00249-008-0274-3)

22 Doster, W., Cusack, S. & Petry, W. 1989 Dynamical transition of myoglobin revealed by inelastic neutron scattering. *Nature* **337**, 754–756. (doi:10.1038/337754a0)

23 Cornicchi, E., Onori, G. & Paciaroni, A. 2005 Picosecond-time-scale fluctuations of proteins in glassy matrices: the role of viscosity. *Phys. Rev. Lett.* **95**, 158104. (doi:10.1103/PhysRevLett.95.158104)

24 Marconi, M., Cornicchi, E., Onori, G. & Paciaroni, A. 2008 Comparative study of protein dynamics in hydrated powders and in solutions: a neutron scattering investigation. *Chem. Phys.* **345**, 224–229. (doi:10.1016/j.chemphys.2007.08.004)

25 Paciaroni, A., Cinelli, S., Cornicchi, E., De Francesco, A. & Onori, G. 2005 Fast fluctuations in protein powders: the role of hydration. *Chem. Phys. Lett.* **410**, 400–403. (doi:10.1016/j.cplett.2005.05.098)

26 Fitter, J. 1999 The temperature dependence of internal molecular motions in hydrated and dry alpha-amylase: the role of hydration water in the dynamical transition of proteins. *Biophys. J.* **76**, 1034–1042. (doi:10.1016/S0006-3495(99)77268-1)

27 Fitter, J. 2003 A measure of conformational entropy change during thermal protein unfolding using neutron spectroscopy. *Biophys. J.* **84**, 3924–3930. (doi:10.1016/S0006-3495(03)75120-0)

28 Fitter, J. & Heberle, J. 2000 Structural equilibrium fluctuations in mesophilic and thermophilic alpha-amylase. *Biophys. J.* **79**, 1629–1636. (doi:10.1016/S0006-3495(00)76413-7)

29 Gabel, F., Bicout, D., Lehnert, U., Tehei, M., Weik, M. & Zaccai, G. 2002 Protein dynamics studied by neutron scattering. *Q. Rev. Biophys.* **35**, 327–367. (doi:10.1017/S0033583502003840)

30 Colombo, M. F., Rau, D. C. & Parsegian, V. A. 1992 Protein solvation in allosteric regulation—a water effect on hemoglobin. *Science* **256**, 655–659. (doi:10.1126/science.1585178)

31 Salvay, A. G., Grigera, J. R. & Colombo, M. F. 2003 The role of hydration on the mechanism of allosteric regulation: *in situ* measurements of the oxygen-linked kinetics of water binding to hemoglobin. *Biophys. J.* **84**, 564–570. (doi:10.1016/S0006-3495(03)74876-0)

32 Schwille, P., Haupts, U., Maiti, S. & Webb, W. W. 1999 Molecular dynamics in living cells observed by fluorescence correlation spectroscopy with one- and two-photon excitation. *Biophys. J.* **77**, 2251–2265. (doi:10.1016/S0006-3495(99)77065-7)

33 Wawrezinieck, L., Rigneault, H., Marguet, D. & Lenne, P. F. 2005 Fluorescence correlation spectroscopy diffusion laws to probe the submicron cell membrane organization. *Biophys. J.* **89**, 4029–4042. (doi:10.1529/biophysj.105.067959)

34 Lal, J., Fouquet, P., Maccarini, M. & Makowski, L. 2010 Neutron spin-echo studies of hemoglobin and myoglobin: multiscale internal dynamics. *J. Mol. Biol.* **397**, 423–435. (doi:10.1016/j.jmb.2010.01.029)

35 Le Coeur, C. & Longeville, S. 2008 Microscopic protein diffusion at high concentration by neutron spin-echo spectroscopy. *Chem. Phys.* **345**, 298–304. (doi:10.1016/j.chemphys.2007.09.042)

36 Antonini, E. & Brunori, M. 1970 Hemoglobin. *Annu. Rev. Biochem.* **39**, 977–1042. (doi:10.1146/annurev.bi.39.070170.004553)

37 Cho, C. H., Urquidi, J., Singh, S. & Wilse Robinson, G. 1999 Thermal offset viscosities of liquid H_2O, D_2O, and T_2O. *J. Phys. Chem. B* **103**, 1991–1994. (doi:10.1021/jp9842953)

38 Tehei, M. *et al.* 2007 Neutron scattering reveals extremely slow cell water in a Dead Sea organism. *Proc. Natl Acad. Sci. USA* **104**, 766–771. (doi:10.1073/pnas.0601639104)

39 Gaspar, A. M., Busch, S., Appavou, M. S., Haeussler, W., Georgii, R., Su, Y. X. & Doster, W. 2010 Using polarization analysis to separate the coherent and incoherent scattering from protein samples. *Biochim. Biophys. Acta Proteins Proteomics* **1804**, 76–82. (doi:10.1016/j.bbapap.2009.06.024)

40 Perez, J., Zanotti, J. M. & Durand, D. 1999 Evolution of the internal dynamics of two globular proteins from dry powder to solution. *Biophys. J.* **77**, 454–469. (doi:10.1016/S0006-3495(99)76903-1)

41 Bee, M. 1988 *Quasielastic neutron scattering. Principles and applications in solid state chemistry, biology and materials science.* Bristol, UK: Adam Hilger.

42 Azuah, R. T., Kneller, L. R., Qiu, Y., Tregenna-Piggott, P. L. W., Brown, C. M., Copley, J. R. D. & Dimeo, R. M. 2009 DAVE: a comprehensive software suite for the reduction, visualization, and analysis of low energy neutron spectroscopic data. *J. Res. Natl. Inst. Stan. Technol.* **114**, 341–358.

43 Gaspar, A. M., Appavou, M. S., Busch, S., Unruh, T. & Doster, W. 2008 Dynamics of well-folded and natively disordered proteins in solution: a time-of-flight neutron scattering study. *Eur. Biophys. J.* **37**, 573–582. (doi:10.1007/s00249-008-0266-3)

44 Unruh, T., Smuda, C., Busch, S., Neuhaus, J. & Petry, W. 2008 Diffusive motions in liquid medium-chain *n*-alkanes as seen by quasielastic time-of-flight neutron spectroscopy. *J. Chem. Phys.* **129**, 121106. (doi:10.1063/1.2990026)

45 Jasnin, M., Moulin, M., Haertlein, M., Zaccai, G. & Tehei, M. 2008 *In vivo* measurement of internal and global macromolecular motions in *E. coli*. *Biophys. J.* **95**, 857–864. (doi:10.1529/biophysj.107.124420)

46 Busch, S., Doster, W., Longeville, S., Garcia Sakai, V. & Unruh, T. 2007 Microscopic protein diffusion at high concentration. In *Proc. Quasi-Elastic Neutron Scattering Conference 2006, Bloomington, IN, 14–17 June 2006* (eds P. E. Sokol, H. Kaiser, D. Baxter, R. Pynn, D. Bossev & M. Leuschner), pp. 107–114. Warrendale, PA: Materials Research Society.

47 Tokuyama, M. & Oppenheim, I. 1994 Dynamics of hard-sphere suspensions. *Phys. Rev. E* **50**, R16–R19. (doi:10.1103/PhysRevE.50.R16)

48 Schelten, J., Schlecht, P., Schmatz, W. & Mayer, A. 1972 Neutron small angle scattering of hemoglobin. *J. Biol. Chem.* **247**, 5436–5441.

49 Svergun, D. I., Richard, S., Koch, M. H., Sayers, Z., Kuprin, S. & Zaccai, G. 1998 Protein hydration in solution: experimental observation by X-ray and neutron scattering. *Proc. Natl Acad. Sci. USA* **95**, 2267–2272. (doi:10.1073/pnas.95.5.2267)

50 DeMoll, E., Cox, D. J., Daniel, E. & Riggs, A. F. 2007 Apparent specific volume of human hemoglobin: effect of ligand state and contribution of heme. *Anal. Biochem.* **363**, 196–203. (doi:10.1016/j.ab.2007.01.035)

51 Stadler, A. M., Embs, J. P., Digel, I., Artmann, G. M., Unruh, T., Buldt, G. & Zaccai, G. 2008 Cytoplasmic water and hydration layer dynamics in human red blood cells. *J. Am. Chem. Soc.* **130**, 16 852–16 853. (doi:10.1021/ja807691j)

52 Garcia de la Torre, J. 2001 Hydration from hydrodynamics. General considerations and applications of bead modelling to globular proteins. *Biophys. Chem.* **93**, 159–170. (doi:10.1016/S0301-4622(01)00218-6)

53 Fitter, J., Lechner, R. E., Buldt, G. & Dencher, N. A. 1996 Internal molecular motions of bacteriorhodopsin: hydration-induced flexibility studied by quasielastic incoherent neutron scattering using oriented purple membranes. *Proc. Natl Acad. Sci. USA* **93**, 7600–7605. (doi:10.1073/pnas.93.15.7600)

54 Fitter, J., Lechner, R. E. & Dencher, N. A. 1997 Picosecond molecular motions in bacteriorhodopsin from neutron scattering. *Biophys. J.* **73**, 2126–2137. (doi:10.1016/S0006-3495(97)78243-2)

55 Orecchini, A., Paciaroni, A., Bizzarri, A. R. & Cannistraro, S. 2002 Dynamics of different hydrogen classes in beta-lactoglobulin: a quasielastic neutron scattering investigation. *J. Phys. Chem. B* **106**, 7348–7354. (doi:10.1021/jp014451x)
56 Volino, F. & Dianoux, A. J. 1980 Neutron incoherent-scattering law for diffusion in a potential of spherical-symmetry—general formalism and application to diffusion inside a sphere. *Mol. Phys.* **41**, 271–279. (doi:10.1080/00268978000102761)
57 Wood, K., Grudinin, S., Kessler, B., Weik, M., Johnson, M., Kneller, G. R., Oesterheit, D. & Zaccai, G. 2008 Dynamical heterogeneity of specific amino acids in bacteriorhodopsin. *J. Mol. Biol.* **380**, 581–591. (doi:10.1016/j.jmb.2008.04.077)
58 Stadler, A. M., Schweins, R., Zaccai, G. & Lindner, P. 2010 Observation of a large-scale superstructure in concentrated hemoglobin solutions by using small angle neutron scattering. *J. Phys. Chem. Lett.* **1**, 1805–1808. (doi:10.1021/jz100576c)
59 Sears, V. F. 1966 Theory of cold neutron scattering by homonuclear diatomic liquids. II. Hindered rotation. *Can. J. Phys.* **44**, 1299–1311.